

Sulfonamido 2 arylbenzoxazole GroEL/ES inhibitors are potent antibacterials against methicillin resistant *Staphylococcus aureus* (MRSA)

AUTHOR NAMES

Sanofar Abdeen,^a Trent Kunkle,^a Nilshad Salim,^a Anne-Marie Ray,^a Najiba Mammadova,^{a,1} Corey Summers,^{a,2} McKayla Stevens,^a Andrew J. Ambrose,^b Yangshin Park,^{a,ef} Peter G. Schultz,^c Arthur L. Horwich,^d Quyen Hoang,^{a,ef} Eli Chapman,^b and Steven M. Johnson^{a,*}

AUTHOR ADDRESSES

a Indiana University School of Medicine, Department of Biochemistry and Molecular Biology, 635 Barnhill Dr., Indianapolis, IN 46202

b The University of Arizona, College of Pharmacy, Department of Pharmacology and Toxicology, 1703 E. Mabel St., PO Box 210207, Tucson, AZ 85721

c The Scripps Research Institute, Department of Chemistry, 10550 North Torrey Pines Rd., La Jolla, CA 92037

d HHMI, Department of Genetics, Yale School of Medicine, Boyer Center for Molecular Medicine, 295 Congress Ave., New Haven, CT 06510

e Stark Neurosciences Research Institute, Indiana University School of Medicine. 320 W. 15th Street, Suite 414, Indianapolis, IN 46202

f Department of Neurology, Indiana University School of Medicine. 635 Barnhill Drive, Indianapolis, IN 46202

PRESENT ADDRESSES

1 Department of Genetics, Development and Cell Biology, Iowa State University, 1210 Molecular Biology Building, Pannel Dr, Ames, IA 50011

2 Department of Kinesiology, Iowa State University, 235 Barbara E. Forker Building, Beach Rd, Ames, IA 50011

KEYWORDS.

GroEL, GroES, HSP60, HSP10, molecular chaperone, chaperonin, proteostasis, small molecule inhibitors, *ESKAPE* pathogens MRSA, antibiotics.

This is the author's manuscript of the article published in final edited form as:

Abdeen, S., Kunkle, T., Salim, N., Ray, A.-M., Mammadova, N., Summers, C., ... Johnson, S. M. (2018). Sulfonamido-2-arylbenzoxazole GroEL/ES inhibitors are potent antibacterials against methicillin-resistant *Staphylococcus aureus* (MRSA). *Journal of Medicinal Chemistry*. <https://doi.org/10.1021/acs.jmedchem.8b00989>

ABSTRACT

1
2
3
4
5
6
7
8
9
10
11
12
13
14
15
16
17
18
19
20
21
22
23
24
25
26
27
28
29
30
31
32
33
34
35
36
37
38
39
40
41
42
43
44
45
46
47
48
49
50
51
52
53
54
55
56
57
58
59
60

Extending from a study we recently published examining the anti-trypanosomal effects of a series of GroEL/ES inhibitors based on a pseudo-symmetrical bis-sulfonamido-2-phenylbenzoxazole scaffold, here, we report the antibiotic effects of asymmetric analogs of this scaffold against a panel of bacteria known as the **ESKAPE** pathogens (*Enterococcus faecium*, *Staphylococcus aureus*, *Klebsiella pneumoniae*, *Acinetobacter baumannii*, *Pseudomonas aeruginosa*, and *Enterobacter* species). While GroEL/ES inhibitors were largely ineffective against *K. pneumoniae*, *A. baumannii*, *P. aeruginosa*, and *E. cloacae* (Gram-negative bacteria), many analogs were potent inhibitors of *E. faecium* and *S. aureus* proliferation (Gram-positive bacteria – EC₅₀ values of the most potent analogs were in the 1-2 μM range). Furthermore, even though some compounds inhibit human HSP60/10 biochemical functions *in vitro* (IC₅₀ values in the 1-10 μM range), many of these exhibited moderate to low cytotoxicity to human liver and kidney cells (CC₅₀ values >20 μM).

INTRODUCTION:

The persistence of antibiotic resistant pathogens is a significant health and economic burden worldwide. Six of the most problematic drug resistant Gram-positive (Gr+) and Gram-negative (Gr-) bacteria are commonly referred to as the **ESKAPE** pathogens. This panel of drug resistant bacteria includes *Enterococcus faecium* (Gr+), *Staphylococcus aureus* (Gr+), *Klebsiella pneumoniae* (Gr-), *Acinetobacter baumannii* (Gr-), *Pseudomonas aeruginosa* (Gr-), and *Enterobacter* species (Gr-).¹⁻⁵ Of particular significance, the CDC recently estimated that ~80,000 individuals are infected with MRSA in the US annually, with ~11,000 deaths – the highest mortality rate amongst all the antibiotic resistant bacteria. *S. aureus*-associated infections range from mild skin infections to life-threatening endocarditis, osteomyelitis, or bacteremia, which are usually treated with penicillinase-resistant beta-lactams or vancomycin. For more resistant strains, newer classes of antibiotics can be prescribed, such as linezolid, daptomycin, dalbavancin, tedizolid.⁶⁻⁸ Unfortunately, despite the availability of several antimicrobials, treating MRSA infections remains a significant challenge owing to off-target toxicities of some antibiotics, lack of efficacy in life-threatening clinical infections such as bacteraemia, endocarditis, etc., and the emergence of pan-drug resistant strains.⁷ Thus, there is an urgent need for new antibacterial drugs that function against previously unexploited targets and pathways to circumvent predisposed resistance mechanisms.

Towards developing mechanistically unique antibacterial candidates, we have focused on exploiting bacterial protein homeostasis pathways. A network of molecular chaperones and proteases collectively functions to maintain protein homeostasis by assisting proteins to fold to their native, functional states, or ensuring their proper degradation and recycling.^{9, 10} Since such

1
2
3 quality control mechanisms are vital to cell survival, targeting them with small molecule
4 inhibitors should be an effective antibacterial strategy. While recent studies have investigated
5 targeting DnaK (a molecular chaperone belonging to the HSP70 family) and Clp proteases,
6 targeting of the bacterial GroEL/GroES chaperonin system has gone largely unexplored.¹¹⁻¹⁴ *E.*
7 *coli* GroEL, which is the prototypical member of the HSP60 chaperonin family of molecular
8 chaperones, is a homo-tetradecameric protein that forms two, seven-subunit rings that stack
9 back-to-back with one another.¹⁵⁻¹⁷ Through a series of events driven by ATP binding and
10 hydrolysis, unfolded substrate polypeptides are bound within the central cavity of a GroEL ring
11 and encapsulated by the GroES co-chaperonin “lid”, allowing protein folding within the
12 sequestered chamber.¹⁷⁻²¹ Since the GroEL/ES chaperonin system is essential for *E. coli* survival
13 under all growth conditions, as it likely is for other bacteria, it represents an excellent target for
14 antibacterial development.^{22, 23} Furthermore, GroEL is highly conserved in prokaryotes
15 (generally >50% sequence identity between bacterial species, whether Gram-positive or Gram-
16 negative), thus, targeting this molecular machinery has the potential for broad spectrum
17 applicability. However, since human HSP60 is also highly conserved (48% identity with *E. coli*
18 GroEL), we also need to consider whether GroEL inhibitors have off-target effects against
19 HSP60 in human cells.

20
21
22
23
24
25
26
27
28
29
30
31
32
33
34
35
36
37
38
39
40
41
42
43
44
45
46
47
48
49
50
51
52
53
54
55
56
57
58
59
60

Towards our goal of exploiting the GroEL/ES chaperonin system as an antibacterial strategy, we previously reported a high-throughput screen that identified 235 small molecule inhibitors of the *E. coli* GroEL/ES chaperonin system.²⁴ In a subsequent study, we evaluated 22 of these GroEL/ES inhibitor hits for their antibacterial properties against the *ESKAPE* pathogens.²⁵ In another study, we evaluated a series of compound **1**-based GroEL/ES inhibitors for their antibiotic effects against *Trypanosoma brucei* parasites – the causative agents of African

1
2
3 sleeping sickness (**Figure 1A**).²⁶ As an extension of those two studies, herein, we have explored
4 additional compound **1** analogs for their ability to selectively inhibit the prototypical *E. coli*
5 GroEL/ES chaperonin system and growth of the *ESKAPE* pathogens over human HSP60/10 and
6 liver and kidney cells. Overall, this study enabled us to better understand the bioactivity profiles
7 of this molecular scaffold, which provided invaluable SAR to guide future studies to more
8 rationally optimize the pharmacological properties of these antibacterial GroEL/ES chaperonin
9 system inhibitors.
10
11
12
13
14
15
16
17
18
19
20

21 **RESULTS AND DISCUSSION**

22 **Identifying preliminary SAR of previously developed pseudo-symmetrical compound **1**** 23 **analogs for antibacterial effects against the *ESKAPE* pathogens.** 24 25

26 From our previous study exploring the antibacterial effects of our different GroEL/ES
27 inhibitor scaffolds, we found that the parent hit, compound **1** (based on the benzimidazole core,
28 **Figure 1A**), exhibited no antibacterial effects against any of the *ESKAPE* pathogens.²⁵
29 Therefore, before embarking on synthesis of new compound **1** analogs, we tested our previously
30 developed benzoxazole-based GroEL/ES inhibitors (compounds **2-14**), which have anti-
31 trypanosomal activities, for their antibacterial properties.²⁶ We expected that this initial
32 evaluation would tell us whether or not this scaffold would be worthwhile to pursue for
33 antibacterial development and, if so, allow us to identify which substituents, substitution
34 patterns, and aryl substructures would provide the most potent antibacterial effects. We
35 employed a standard antibacterial efficacy assay in liquid culture as previously reported, with
36 one modification: the media was cation-adjusted by addition of 25 mg/L Ca²⁺ and 12.5 mg/L
37 Mg²⁺ to better mimic the concentrations of these divalent cations *in vivo*, which can alter the
38
39
40
41
42
43
44
45
46
47
48
49
50
51
52
53
54
55
56
57
58
59
60

1
2
3 antibacterial effects of some compounds (e.g. daptomycin is a more potent inhibitor when media
4 is supplemented with additional Ca^{2+} and Mg^{2+} ions).²⁷ Briefly, bacteria were grown at 37°C
5
6 without shaking (stagnant assay) in media stamped with test compounds. Compounds were first
7
8 tested at single concentrations of 100 μM , then in dose-response for those that exhibited >50%
9
10 inhibition of bacterial proliferation (refer to **Tables S1A** and **S2A** in the Supporting Information
11
12 for a tabulation of all EC_{50} results). After 6-8 h (*S. aureus*, MRSA, *K. pneumonia*, *E. cloacae*,
13
14 and *P. aeruginosa*) or 24 h (*E. faecium* and *A. baumannii*), the absorbance of each well was read
15
16 at 600 nm to monitor turbidity from bacterial growth, from which EC_{50} results were obtained by
17
18 plotting the dose-response measurements and fitting data with non-linear regression. A detailed
19
20 protocol for this assay is listed in the Supporting Information.
21
22
23
24
25

26 Preliminary results from these proliferation assays indicated that all but one compound
27
28 (**2h-p**) were inactive against the four Gram-negative *KAPE* bacterial species, and only three were
29
30 able to inhibit *E. faecium* (the *ortho*-, *meta*-, and *para*-substituted analogs of hydroxylated
31
32 compound **2h**); however, several compounds were able to inhibit *S. aureus* and MRSA
33
34 proliferation (**Figure 1B**, and **Tables S1A** and **S2A** in the Supporting Information). Furthermore,
35
36 these compounds were reasonably selective at killing MRSA in relation to their cytotoxicity
37
38 CC_{50} values obtained from liver (THLE 3) and kidney (HEK 293) cell viability assays, which
39
40 were determined in the previous study targeting *T. brucei* parasites.²⁶ Preliminary SAR revealed
41
42 that the sulfonamide end-capping thiophene and *para*-chlorophenyl groups gave the most potent
43
44 and selective aryl and substituent/substitution patterns, respectively (**Figure 1B**). Based on these
45
46 initial results, we decided to combine these two moieties, reasoning that inhibition properties of
47
48 each could be additive, and developed two parallel series of 2-chlorothiophene-based
49
50
51
52
53
54
55
56
57
58
59
60

1
2
3 asymmetrical analogs (**Figure 1C**, analogs **15-34**) containing variable substructures at the **R**²
4 positions.
5
6
7
8
9

10 **Synthesis of the two parallel series of 2-chlorothiophene-based analogs.**

11
12 We rationalized that the previously developed pseudo-symmetrical compound **1** analogs
13 (i.e. with the same sulfonamide end-capping substructures on either side of the molecules) may
14 not be truly optimized for binding to and inhibiting the chaperonin system. Thus, to better
15 complement the envisioned asymmetric binding sites, we designed two parallel series of analogs
16 with a variety of alkyl and aryl substructures at the **R**² positions on the **Right (R-series)** and **Left**
17 (**L-series**) sides of the 2-phenylbenzoxazole scaffold, while keeping the 2-
18 chlorothiophenesulfonamide moiety on the opposite sides (**Figure 1C**). The same **R**²-groups
19 were used to create the panel of 19 matched-pairs for the different **R-** and **L-series** analogs, with
20 an additional pseudo-symmetrical analog (**15**) that contained the 2-chlorothiophenesulfonamide
21 on both sides (thus, a total of 39 new compounds were synthesized for evaluation). We expected
22 that these matched pairs of analogs would help us to identify whether or not the directionality of
23 the 2-phenylbenzoxazole core would significantly impact inhibitor effects in the various
24 biochemical and cell-based assays they would be tested in. The general syntheses of these
25 analogs are shown in **Scheme 1**, with detailed procedures and compound characterizations
26 presented in the Experimental section and Supporting Information. Each of the **R-** and **L-series**
27 of analogs were synthesized through 5-step linear protocols employing facile reactions. All final
28 test compounds were characterized by ¹H-NMR and LC-MS analyses for structural confirmation,
29 and by two independent sets of HPLC conditions for purity identification (all were >95% pure
30 under both conditions).
31
32
33
34
35
36
37
38
39
40
41
42
43
44
45
46
47
48
49
50
51
52
53
54
55
56
57
58
59
60

1
2
3 For synthesizing the **R**-series analogs, 2-chlorothiophenesulfonyl chloride was first
4 coupled to 4-amino-2-nitrophenol in dichloromethane using pyridine as base, giving **35**.^{26, 28, 29}
5
6 Reduction of the nitro group was accomplished by reacting with tin powder in a 1:10 v/v mixture
7 of hydrochloric acid in glacial acetic acid.²⁸⁻³⁰ Next, an intermediate Schiff base was formed by
8 refluxing **36** and *para*-nitrobenzaldehyde with sodium bicarbonate in anhydrous THF, which was
9 then cooled and cyclized to benzoxazole **37** by addition of DDQ.³¹ The nitro group was again
10 reduced using tin powder in HCl/AcOH, affording intermediate **38**, from which the final bis-
11 sulfonamido analogs (**15** and **16R-34R**) could be rapidly generated by coupling with a variety of
12 differentially-substituted sulfonyl chlorides (**R**²-SO₂Cl).
13
14
15
16
17
18
19
20
21
22
23

24 For synthesizing the **L**-series analogs, 2-chlorothiophenesulfonyl chloride was first
25 coupled to methyl-4-aminobenzoate in dichloromethane using pyridine as base, giving **39**. The
26 ester was then hydrolyzed with LiOH in a mixture of H₂O/MeOH/THF, affording acid **40**.^{28, 30, 32}
27
28 The acid was then converted to the acyl chloride, concentrated, and coupled to 2-amino-4-
29 nitrophenol in dichloromethane with pyridine as base, affording the intermediate amide, which
30 was then cyclodehydrated to **41** by refluxing with toluenesulfonic acid in xylenes.^{29, 33} The nitro
31 group was subsequently reduced with tin powder in HCl/AcOH, affording intermediate **42**, from
32 which the final bis-sulfonamido analogs (**16L-34L**) could be rapidly generated by coupling with
33 a variety of differentially-substituted sulfonyl chlorides (**R**²-SO₂Cl).
34
35
36
37
38
39
40
41
42
43
44
45
46

47 **Evaluating compounds for antibiotic effects against the *ESKAPE* bacteria and inhibition of** 48 **GroEL/ES-mediated folding of substrate proteins.** 49

50
51 Before proceeding with extensive biochemical and biophysical characterization of the
52 new 2-chlorothiophene-based analogs, we first tested for their antibiotic effects on the *ESKAPE*
53
54
55
56
57
58
59
60

1
2
3 bacteria using the proliferation assay described above (refer to **Tables S3A** and **S4A** in the
4 Supporting Information for tabulations of all EC₅₀ results). Much like the initial testing with the
5 pseudo-symmetrical analogs, all but one of the 2-chlorothiophene analogs were inactive against
6 the four Gram-negative *KAPE* bacterial species (**27R** had an EC₅₀ of 37 μM against *A.*
7 *baumannii*). However, 14 of the 39 new analogs (36%) exhibited antibacterial effects against *E.*
8 *faecium*, compared to 3 out of 50 (6%) of the pseudo-symmetrical compounds. What was
9 particularly impressive was that 27 out of the 39 new analogs (69%) inhibited *S. aureus* and
10 MRSA, with greater overall potency, compared to the 20 out of 50 (40%) of the pseudo-
11 symmetrical compounds (**Figure 2A** presents a correlation plot of EC₅₀ values for each
12 compound determined in these two assays). To compare assay results between the **R-** and **L-**
13 series analogs, we analyzed the log(EC₅₀) values of each data set using two-tailed, paired t-tests
14 (95% confidence level) and looked at differences between paired values (results are plotted in
15 **Figure S1** in the Supporting Information). For the *E. faecium* EC₅₀ results, we did not see a
16 statistical difference between results from the **R-** and **L-**series analogs (**Figure S1A**). However,
17 there was a statistically significant difference between results of the two series for inhibiting *S.*
18 *aureus* and MRSA proliferation, with the **L-**series generally providing more potent inhibitors of
19 bacterial proliferation for each strain (**Figures S1B** and **S1C**). Although exceptions are evident
20 for individual compounds, there was no statistical difference between inhibiting the drug
21 susceptible *S. aureus* and MRSA strains when the data sets were analyzed for all 89 compounds
22 as a whole (**Figure S5A**).

23
24
25
26
27
28
29
30
31
32
33
34
35
36
37
38
39
40
41
42
43
44
45
46
47
48
49 Having ascertained that the majority of the **R-** and **L-**series analogs were potent inhibitors
50 of *S. aureus* and MRSA proliferation, we next evaluated their abilities to inhibit the biochemical
51 function of the GroEL/ES chaperonin system. For this, we employed our previously reported
52
53
54
55
56
57
58
59
60

1
2
3 assays that monitor GroEL/ES-mediated refolding of two denatured substrate enzymes, malate
4 dehydrogenase (dMDH) and rhodanese (dRho).²⁵ Since these were coupled assays that monitor
5
6 chaperonin-mediated refolding of substrates by virtue of the enzymatic activities of the refolded
7
8 substrates, we further counter-screened against the native MDH and Rho enzymes to ensure that
9
10 compounds were not simply false-positives of the reporter reactions. Detailed protocols for these
11
12 assays and tabulation of all IC₅₀ results are presented in the Supporting Information.
13
14
15

16
17 Because the previously developed pseudo-symmetrical analogs (**1-14**) were not tested in
18
19 the GroEL/ES-dRho refolding assay, nor the native rhodanese enzymatic reporter reaction
20
21 counter screen, we also evaluated those compounds in these two assays. When looking at all 89
22
23 compounds as a whole, although a correlation is evident, we noticed a statistically significant
24
25 difference between the GroEL/ES-dMDH and GroEL/ES-dRho refolding IC₅₀ results (**Figures**
26
27 **2B** and **S5B**), where compounds were slightly more potent at inhibiting GroEL/ES-mediated
28
29 refolding of denatured MDH. This difference does not appear to be a result of compounds
30
31 preferentially inhibiting the native MDH reporter enzyme over rhodanese – while eleven analogs
32
33 inhibited the native MDH enzymatic reporter reaction, five inhibited native rhodanese, and only
34
35 to a minor extent. Since only one compound inhibits both native malate dehydrogenase and
36
37 native rhodanese (**28R**), and only to a minor extent, this supports that compounds are on-target
38
39 for inhibiting the GroEL/ES-mediated folding cycle.
40
41
42
43

44
45 For the purposes of categorizing inhibitor potencies in the GroEL/ES-mediated refolding
46
47 assays, we consider compounds with IC₅₀ values >100 μM to be inactive, 30-100 μM to be weak
48
49 inhibitors, 10-30 μM moderate inhibitors, 1-10 μM potent inhibitors, and <1 μM very potent and
50
51 acting near stoichiometrically since the concentration of GroEL tetradecamer is 50 nM during
52
53 the refolding cycle (i.e. 700 nM of GroEL subunits). Upon further dissection of the GroEL/ES-
54
55
56
57
58
59
60

1
2
3 dMDH refolding assay IC_{50} results, we observed that the asymmetric **R**- and **L**-series analogs are
4 generally more potent than the previously developed pseudo-symmetric analogs: 28 out of 38
5 (74%) of the asymmetric **R**- and **L**-series analogs (**16-34**) have IC_{50} values less than 10 μ M,
6 whereas only 16 out of 51 (31%) of the pseudo-symmetric analogs (**1-15**) have IC_{50} values less
7 than 10 μ M. These results are not entirely surprising since the **R**- and **L**-series analogs were
8 hypothesized to better complement the envisioned asymmetric binding sites than the pseudo-
9 symmetric compounds. However, we caution on over-interpreting these results since the analog
10 groupings did contain different alkyl and aryl substructures on the sulfonamide end-caps. When
11 comparing the **R**- and **L**-series analogs with each other, though, we do not see any statistically
12 significant differences in either the GroEL/ES-dMDH or GroEL/ES-dRho refolding assay results
13 (**Figure S2A and S2B**), suggesting that the orientation of the 2-phenylbenzoxazole core scaffold
14 does not play a significant factor in these compounds binding to and inhibiting the GroEL/ES
15 chaperonin system.
16
17
18
19
20
21
22
23
24
25
26
27
28
29
30
31
32

33 When comparing IC_{50} results for compounds tested in the biochemical GroEL/ES-dMDH
34 refolding assay with EC_{50} results for testing in the *S. aureus* proliferation assay (**Figure 2C** and
35 **Tables S3A-B and S4A-B**), we note that no compounds are active against bacteria unless they
36 are able to inhibit GroEL. In general, the more potent compounds are at inhibiting the GroEL/ES
37 chaperonin system, the more potent their antibacterial effects, in particular for the **L**-series
38 inhibitors. However, several exceptions are evident where potent GroEL/ES inhibitors are
39 poorly effective, or ineffective, against bacteria, which may owe to poor cell wall permeability
40 and/or efflux, as we had previously observed for other GroEL/ES inhibitor scaffolds.²⁵ Also,
41 while correlations between biochemical IC_{50} and cell-based EC_{50} are only suggestive of
42 mechanisms of action in cells, they are not confirmatory. Thus, whether compounds are “on-
43
44
45
46
47
48
49
50
51
52
53
54
55
56
57
58
59
60

1
2
3 target” for GroEL within bacteria is still unknown and warrants further investigation. These
4
5 studies are ongoing and will be reported in the future.
6
7
8
9

10 **Characterizing GroEL-inhibitor binding interactions using Isothermal Titration**

11 **Calorimetry.**

12
13
14 To further interrogate inhibitor mechanisms of action against GroEL, we used isothermal
15 titration calorimetry (ITC) to identify the thermodynamic parameters, binding affinities, and
16 binding stoichiometries of compounds **20R** and **20L**. While these two compounds were only
17 moderately active at inhibiting *S. aureus* and MRSA proliferation, they were strong inhibitors of
18 GroEL/ES-mediated folding functions, and thus likely had high binding affinities. Furthermore,
19 because they bore primary amines that would be charged under physiological conditions, they
20 were much more soluble than other inhibitors and thus more amenable to ITC analysis, which
21 requires high concentrations of both protein and ligands in matched aqueous buffers. We
22 performed ITC analyses by titrating 400 μM GroEL (monomer concentration) into solutions
23 containing either 50 μM **20R** or **20L** (detailed protocols are presented in the Experimental
24 section). Two representative isotherms for the binding of **20R** and **20L** to GroEL are presented
25 in **Figure 3**. After subtraction of background heats of mixing and dilution, plots of the integrated
26 heats from compound binding fit well to a single-site binding model.³⁴ Averaged results for the
27 various binding parameters (K_d , n , ΔH , ΔS , and ΔG) obtained from replicate analyses (six
28 replicates for **20R**, and five replicates for **20L**) are presented in **Table 1**.
29
30
31
32
33
34
35
36
37
38
39
40
41
42
43
44
45
46
47
48

49 From the averaged results, we found that **20R** had a K_d of 36 nM for binding to *E. coli*
50 GroEL, while the K_d of **20L** was about four-fold higher (150 nM), which corresponds reasonably
51 well with the relative IC_{50} values for inhibiting GroEL/ES-mediated refolding of dMDH and
52
53
54
55
56
57
58
59
60

1
2
3 dRho – the IC₅₀ values for **20L** were typically two- to four-fold higher than for **20R**. For both
4
5 compounds, binding was predominantly enthalpically driven, with minor entropic contributions
6
7 to affinity. What was particularly interesting from these analyses was the stoichiometry of
8
9 binding of each compound to GroEL. Since GroEL consists of 14 identical subunits, we
10
11 anticipated that compounds could bind with a stoichiometry of 14, or potentially 7 if there is
12
13 negative cooperativity between the two GroEL rings (also assuming that for inhibitor binding
14
15 there is no negative cooperativity between subunits within a ring). Since IC₅₀ values were
16
17 previously found to correlate between GroEL/ES-mediated refolding and ATPase assays for this
18
19 inhibitor scaffold, the most likely binding sites may be the ATP pockets, of which there are 1 per
20
21 GroEL subunit (14 per oligomer).²⁶ However, **20R** bound with a stoichiometry of roughly 18
22
23 molecules per GroEL tetradecamer, and **20L** with 23 molecules, which could indicate more than
24
25 one potential binding site per GroEL subunit, and potentially an unknown site outside of the ATP
26
27 pockets. We are currently pursuing X-ray crystallographic studies to identify specific inhibitor
28
29 binding sites, which we will report on in future studies.
30
31
32
33
34
35
36
37

38 **Counter-screening compounds for inhibition of HSP60/10-mediated refolding of denatured** 39 **MDH and for cytotoxicity in human cell viability assays.**

40
41
42 Having established that the **R**- and **L**-series analogs were potent GroEL/ES chaperonin
43
44 system inhibitors with anti-staphylococcal properties, we next investigated their selectivity
45
46 profiles compared to the human HSP60/10 chaperonin system. For this, we evaluated
47
48 compounds in our previously reported HSP60/10-dMDH refolding assay, which is analogous to
49
50 that used for determining inhibition of bacterial GroEL/ES, but alternatively employs the human
51
52 chaperonin system. A detailed protocol and tabulation of all IC₅₀ results for this assay are
53
54
55
56
57
58
59
60

1
2
3 presented in the Supporting Information. We previously reported that the pseudo-symmetrical
4 analogs (**1-14**) were highly selective for inhibiting *E. coli* GroEL/ES over human HSP60/10
5
6 (**Figure 3A and S3A**).²⁶ However, for the asymmetric compounds developed in this study,
7
8 selectivity for inhibiting GroEL/ES over HSP60/10 was statistically significant for the **R**-series
9
10 analogs (**Figure S3C**), but was lost for the **L**-series analogs (**Figure S3B**). Correspondingly,
11
12 differences in IC₅₀ values between the **R**- and **L**-series inhibitors in the HSP60/10-dMDH
13
14 refolding assay were statistically significant (**Figure S4A**), which suggests that directionality of
15
16 the 2-phenylbenzoxazole core does have an effect on compounds binding to and inhibiting the
17
18 human chaperonin system, unlike the situation for *E. coli* GroEL/ES.
19
20
21
22
23

24 We next evaluated the cytotoxicity of our compounds to human liver (THLE 3) and
25
26 kidney (HEK 293) cell lines in a well-established, 48 h, Alamar Blue-based cell viability assay.
27
28 Detailed protocols and tabulation of all cytotoxicity CC₅₀ results for these assays are presented in
29
30 the Supporting Information. Intriguingly, even though the **L**-series analogs are more potent
31
32 HSP60/10 inhibitors than the **R**-series, we observed no statistically significant differences
33
34 between the **L**- and **R**-series CC₅₀ values in the HEK 293 kidney cell viability assay (**Figure**
35
36 **S4B**). Furthermore, we observed an opposing trend where the **L**-series was less cytotoxic to the
37
38 THLE 3 liver cells compared to the **R**-series analogs, although the differences were small
39
40 (**Figure S4B & C**). These results suggest that the compounds may be unable to penetrate the
41
42 mitochondrial matrix to engage with the HSP60/10 chaperonin system, and instead may be
43
44 interacting with other targets in the cytosol or other sub-cellular compartments; however, we
45
46 have yet to confirm this hypothesis. What is particularly promising with these results is that the
47
48 cytotoxicity of lead analogs has not concomitantly increased as with antibacterial potency.
49
50
51
52
53
54 Compared to the previously developed pseudo-symmetrical analogs, several lead asymmetrical
55
56
57
58
59
60

1
2
3 analogs have appreciably higher Selectivity Indices (SI) for inhibiting MRSA proliferation over
4 cytotoxicity in the liver cell viability assay (**Figure 4C**). The biochemical and cell-based IC_{50} ,
5 EC_{50} , and CC_{50} results for the top four lead inhibitors of the pseudo-symmetrical, **R**-series, and
6 **L**-series analogs are presented in **Table 2**, ranked based on their selectivity indices. Notably,
7
8 compounds **24L** and **25L** have selectivity indices of 31 and 46, respectively.
9
10
11
12
13
14
15
16

17 **Investigating the potential for MRSA to gain resistance to lead inhibitors.**

18
19 While selectivity indices (and therapeutic windows with regards to *in vivo* evaluation) are
20 important criteria to consider for antibacterial development, it is also important to determine
21 whether or not bacteria will be able to rapidly develop resistance to lead candidates, especially if
22 they function through new mechanisms of action. To gauge the efficacy of our GroEL/ES
23 inhibitors for eluding acute antibacterial resistance mechanisms, we performed a step-wise,
24 liquid culture resistance assay by consecutively passaging the MRSA strain (ATCC BAA-44) for
25 12 cycles over 12 consecutive days in the presence of serially-diluted inhibitors **20R**, **28R**, and
26 vancomycin for comparison (a detailed protocol is presented in the Experimental section).^{35, 36}
27
28 At the end of each cycle (i.e. each 24 h passage), EC_{50} values were determined for the test
29 compounds, with the assumption that EC_{50} values would increase over time if MRSA was able to
30 generate acute resistance. A plot of test compound EC_{50} values over time is presented in **Figure**
31
32 **5A**. Despite the fact that **28R** was a potent MRSA growth inhibitor (initial EC_{50} value of 1.7
33 μ M), the bacteria rapidly developed resistance to compound concentrations in excess of 100 μ M.
34
35 However, after culturing in the absence of inhibitors for two days (24 h on agar, and another 24 h
36 in liquid media), bacteria regained sensitivity to **28R** (**Figure 5B**), suggesting resistance is
37
38 reversible, potentially from up-regulation of efflux pumps. Most importantly, we found that the
39
40
41
42
43
44
45
46
47
48
49
50
51
52
53
54
55
56
57
58
59
60

1
2
3 parent MRSA strain was unable to generate resistance against **20R** over the 12 day passage, even
4
5 though this analog was only a moderate inhibitor of MRSA proliferation ($EC_{50} = 19 \mu\text{M}$). These
6
7 results suggest that pan-resistance to these GroEL inhibitor analogs may be difficult to develop,
8
9 which supports the continued optimization of lead antibacterial candidates based on this
10
11 molecular scaffold.
12
13

14 15 16 17 CONCLUSIONS. 18

19 From exploratory screening of the antibacterial effects of our previously reported pseudo-
20
21 symmetrical compound **1** analogs,²⁶ we were able to develop two parallel **R**- and **L**-series of 2-
22
23 chlorothiophene-based asymmetrical analogs with significantly improved antibacterial efficacy
24
25 profiles against MRSA. While there were no statistical differences between either the **R**- or **L**-
26
27 series analogs for inhibiting in the GroEL/ES-mediated refolding assays, the **L**-series analogs
28
29 were found to be more potent at inhibiting *S. aureus* and MRSA proliferation – i.e. preferred
30
31 from an antibiotic development perspective (**Table 3**). While a general trend is observed
32
33 between inhibitor potencies in the biochemical GroEL/ES-dMDH refolding assay and the MRSA
34
35 proliferation assay (in particular for the **L**-series analogs), further studies are needed to
36
37 conclusively determine whether or not inhibitors are on-target in bacteria. Using ITC to
38
39 characterize the binding interactions between GroEL and inhibitors **20R** and **20L**, we found that
40
41 inhibitor binding was predominantly enthalpically driven. Furthermore, we observed that >14
42
43 molecules were bound per GroEL tetradecamer (i.e. more than one molecule bound per GroEL
44
45 subunit), suggesting that inhibitors could be binding to unknown sites outside of the ATP
46
47 pockets. Current studies are underway to identify and characterize these putative binding sites so
48
49 that more rigorous structure-based optimization of lead candidates can be conducted. Even
50
51
52
53
54
55
56
57
58
59
60

1
2
3 though the **R**-series analogs were overall less potent at inhibiting HSP60/10, the **L**-series was
4 less cytotoxic against the human liver cells tested, and is likely preferential for further
5
6 antibacterial optimization going forward. However, before pursuing *in vivo* development of this
7
8 series, further medicinal chemistry optimization is warranted to increase the selectivity indices
9
10 for killing MRSA over cytotoxicity to human cells.
11
12
13

14 15 16 17 **EXPERIMENTAL.**

18 19 **General Synthetic Methods.**

20
21 Unless otherwise stated, all chemicals were purchased from commercial suppliers and
22 used without further purification. Reaction progress was monitored by thin-layer
23
24 chromatography on silica gel 60 F254 coated glass plates (EM Sciences). Flash chromatography
25
26 was performed using a Biotage Isolera One flash chromatography system and eluting through
27
28 Biotage KP-Sil Zip or Snap silica gel columns for normal-phase separations (hexanes:EtOAc
29
30 gradients), or Snap KP-C18-HS columns for reverse-phase separations (H₂O:MeOH gradients).
31
32 Reverse-phase high-performance liquid chromatography (RP-HPLC) was performed using a
33
34 Waters 1525 binary pump, 2489 tunable UV/Vis detector (254 and 280 nm detection), and 2707
35
36 autosampler. For preparatory HPLC purification, samples were chromatographically separated
37
38 using a Waters XSelect CSH C18 OBD prep column (part number 186005422, 130 Å pore size,
39
40 5 µm particle size, 19x150 mm), eluting with a H₂O:CH₃CN gradient solvent system. Linear
41
42 gradients were run from either 100:0, 80:20, or 60:40 A:B to 0:100 A:B (A = 95:5 H₂O:CH₃CN,
43
44 0.05% TFA; B = 5:95 H₂O:CH₃CN, 0.05% TFA. Products from normal-phase separations were
45
46 concentrated directly, and reverse-phase separations were concentrated, diluted with H₂O,
47
48 frozen, and lyophilized. For primary compound purity analyses (HPLC-1), samples were
49
50
51
52
53
54
55
56
57
58
59
60

1
2
3 chromatographically separated using a Waters XSelect CSH C18 column (part number
4 186005282, 130 Å pore size, 5 µm particle size, 3.0x150 mm), eluting with the above
5
6 H₂O:CH₃CN gradient solvent systems. For secondary purity analyses (HPLC-2) of final test
7
8 compounds, samples were chromatographically separated using a Waters XBridge C18 column
9
10 (either part number 186003027, 130 Å pore size, 3.5 µm particle size, 3.0x100 mm, or part
11
12 number 186003132, 130 Å pore size, 5.0 µm particle size, 3.0x100 mm), eluting with a
13
14 H₂O:MeOH gradient solvent system. Linear gradients were run from either 100:0, 80:20, 60:40,
15
16 or 20:80 A:B to 0:100 A:B (A = 95:5 H₂O:MeOH, 0.05% TFA; B = 5:95 H₂O:MeOH, 0.05%
17
18 TFA). Test compounds were found to be >95% in purity from both RP-HPLC analyses. Mass
19
20 spectrometry data were collected using either an Agilent analytical LC-MS at the IU Chemical
21
22 Genomics Core Facility (CGCF), or a Thermo-Finnigan LTQ LC-MS in-lab. ¹H-NMR spectra
23
24 were recorded on either Bruker 300 MHz or 500 MHz spectrometers. Chemical shifts are
25
26 reported in parts per million and calibrated to the *d*₆-DMSO solvent peaks at 2.50 ppm. We
27
28 previously synthesized compounds **1-14** (including **2a-m-o/m/p**)²⁶ and re-synthesized where
29
30 necessary due to stock depletion. Synthesis and characterization of intermediates **35-42** are
31
32 presented below. General sulfonamide coupling steps are presented for analogs **15** and **16R-34R**
33
34 and **16L-34L** below, with compound characterizations for each analog presented in the
35
36 Supporting Information.
37
38
39
40
41
42
43
44
45
46

47 **35: 5-Chloro-*N*-(4-hydroxy-3-nitrophenyl) thiophene-2-sulfonamide.**

48
49 To a stirring mixture of 4-amino-2-nitrophenol (5.34 g, 24.6 mmol) in anhydrous CH₂Cl₂
50
51 (50 mL) was added 5-chlorothiophene-2-sulfonyl chloride (4.21 g, 27.3 mmol) and pyridine
52
53 (2.40 mL, 29.4 mmol). The reaction was allowed to stir at room temperature for 18 h and was
54
55
56
57
58
59
60

1
2
3 then diluted with hexanes and the precipitate was filtered, rinsed with 1 M HCl and water,
4
5 collected, and dried to afford **35** as a reddish-brown solid (7.70 g, 94% yield). ¹H-NMR (300
6
7 MHz, *d*₆-DMSO) δ 10.98 (br s, 1H), 10.62 (br s, 1H), 7.60 (d, *J* = 2.7 Hz, 1H), 7.39 (d, *J* = 4.1
8
9 Hz, 1H), 7.30 (dd, *J* = 8.9, 2.7 Hz, 1H), 7.22 (d, *J* = 4.1 Hz, 1H), 7.10 (d, *J* = 8.9 Hz, 1H); MS
10
11 (ESI) C₁₀H₆ClN₂O₅S₂ [M-H]⁻ *m/z* expected = 332.9, observed = 332.8; HPLC-1 = >99% (RT =
12
13 8.1 min).
14
15
16
17
18

19 **36: *N*-(3-Amino-4-hydroxyphenyl)-5-chlorothiophene-2-sulfonamide.**

20
21 Tin powder (8.73 g, 73.6 mmol) was added slowly to a stirring mixture of **35** (8.11 g,
22
23 24.2 mmol) in a 1:10 mixture of HCl:AcOH (24 mL). The reaction was allowed to stir at R.T.
24
25 for 18 h, then diluted with EtOAc and H₂O, neutralized with NaHCO₃, and filtered. The filtrate
26
27 was extracted with EtOAc and the organics dried over Na₂SO₄, filtered, and concentrated. The
28
29 residue was diluted in a 50% mixture of DCM in hexanes and the precipitate was filtered, rinsed
30
31 with hexanes, collected, and dried to afford **36** as a brown powder (6.08 g, 82% yield). ¹H-NMR
32
33 (300 MHz, *d*₆-DMSO) δ 9.81 (br s, 1H), 8.99 (br s, 1H) 7.28 (d, *J* = 4.1 Hz, 1H), 7.18 (d, *J* = 4.1
34
35 Hz, 1H), 6.49 (d, *J* = 8.3 Hz, 1H), 6.41 (d, *J* = 2.5 Hz, 1H), 6.13 (dd, *J* = 8.3, 2.6 Hz, 1H), 4.64
36
37 (br s, 2H); MS (ESI) C₁₀H₁₀ClN₂O₃S₂ [M+H]⁺ *m/z* expected = 305.0, observed = 304.9; HPLC-1
38
39 = 97% (RT = 6.0 min).
40
41
42
43
44
45
46

47 **37: 5-Chloro-*N*-(2-(4-nitrophenyl)benzo[d]oxazol-5-yl)thiophene-2-sulfonamide.**

48
49 Compound **36** (2.94 g, 9.65 mmol), 4-nitrobenzaldehyde (2.03 g, 13.4 mmol), NaHCO₃
50
51 (2.08 g, 24.8 mmol), and Na₂SO₄ (3.35 g) were stirred in THF (40 mL) for 4 h at reflux (under
52
53 Ar), then cooled to R.T. DDQ (2.85 g, 12.6 mmol) was then add portion-wise and the reaction
54
55
56
57
58
59
60

1
2
3 was left to stir for 2 h, then filtered. The filtrate was extracted into EtOAc, rinsed with saturated
4 NaHCO₃, 1 M HCl, and brine. The organics layer was dried over Na₂SO₄, filtered, and
5 concentrated. The residue was diluted in a 25% mixture of DCM in hexanes and the precipitate
6 was filtered, rinsed with hexanes, collected, and dried to afford **37** as a brown powder (4.01 g,
7 95% yield). ¹H-NMR (300 MHz, *d*₆-DMSO) δ 10.74 (s, 1H), 8.37-8.48 (m, 4H), 7.82 (d, *J* = 8.8
8 Hz, 1H), 7.60 (d, *J* = 1.9 Hz, 1H), 7.43 (d, *J* = 4.0 Hz, 1H), 7.25 (dd, *J* = 8.8, 2.1 Hz, 1H), 7.19
9 (d, *J* = 4.1 Hz, 1H); MS (ESI) C₁₇H₉ClN₃O₅S₂ [M-H]⁻ *m/z* expected = 434.0, observed = 433.8;
10 HPLC-1 = 91% (RT = 7.7 min).
11
12
13
14
15
16
17
18
19
20
21
22
23

24 **38: *N*-(2-(4-Aminophenyl)benzo[d]oxazol-5-yl)-5-chlorothiophene-2-sulfonamide.**

25
26 Tin powder (2.74 g, mmol) was added slowly to a stirring mixture of **37** (2.43 g, 5.58
27 mmol) in a 1:10 mixture of HCl:AcOH (15 mL). The reaction was allowed to stir at R.T. for 18
28 h, then diluted with EtOAc and H₂O, neutralized with NaHCO₃, and filtered. The filtrate was
29 extracted with EtOAc and the organics dried over Na₂SO₄, filtered, and concentrated. The
30 residue was chromatographed over silica (hexanes:EtOAc gradient) and concentrated to afford
31 **38** as an orange solid (936 mg, 41% yield). ¹H-NMR (300 MHz, *d*₆-DMSO) δ 10.54 (s, 1H),
32 7.78-7.86 (m, 2H), 7.60 (d, *J* = 8.7 Hz, 1H), 7.35-7.40 (m, 2H), 7.18 (d, *J* = 4.1 Hz, 1H), 7.04
33 (dd, *J* = 8.6, 2.2 Hz, 1H), 6.64-6.71 (m, 2H), 6.04 (br s, 2H); MS (ESI) C₁₇H₁₃ClN₃O₃S₂ [M+H]⁺
34 *m/z* expected = 406.0, observed = 405.9; HPLC-1 = 97% (RT = 7.6 min).
35
36
37
38
39
40
41
42
43
44
45
46
47
48

49 **General sulfonamidation procedure for the synthesis of 16R-34R.**

50
51 To a stirring mixture of compound **38** (1 eq.) in anhydrous CH₂Cl₂ (5 mL) was added the
52 respective **R**² sulfonyl chloride (1.2 eq.) followed by anhydrous pyridine (1.2 eq.). The reaction
53
54
55
56
57
58
59
60

1
2
3 was allowed to stir at room temperature for 18 h and was then chromatographed over silica
4 (hexanes:EtOAc gradient) and concentrated. If necessary, the product was further purified by
5 preparatory RP-HPLC (H₂O:CH₃CN gradient), concentrated, and lyophilized. Refer to the
6
7 Supporting Information for individual compound characterization data.
8
9
10
11
12
13

14
15 **39: Methyl 4-((5-chlorothiophene)-2-sulfonamido)benzoate.**
16

17 To a stirring mixture of methyl-4-aminobenzoate (2.76 g, 18.3 mmol) in anhydrous
18 CH₂Cl₂ (50 mL) was added 5-chlorothiophene-2-sulfonyl chloride (4.78 g, 22.0 mmol) and
19 pyridine (1.80 mL, 22.1 mmol). The reaction was allowed to stir at room temperature for 18 h
20 and was then diluted with hexanes and acidified with 1 M HCl. The precipitate was then filtered,
21 rinsed with 1 M HCl and water, collected, and dried to afford **39** as a pinkish-orange solid (5.94
22 g, 98% yield). ¹H-NMR (300 MHz, *d*₆-DMSO) δ 11.16 (br s, 1H), 7.86-7.93 (m, 2H), 7.56 (d, *J*
23 = 4.1 Hz, 1H), 7.25-7.31 (m, 2H), 7.22 (d, *J* = 4.1 Hz, 1H), 3.80 (s, 3H); HPLC-1 = 99% (RT =
24 6.2 min).
25
26
27
28
29
30
31
32
33
34
35
36
37

38 **40: 4-((5-Chlorothiophene)-2-sulfonamido)benzoic acid.**
39

40 LiOH·H₂O (7.02 g, 167 mmol) was added to a stirring mixture of **39** (5.67 g, 17.1 mmol)
41 in THF (20 mL), MeOH (20 mL), and H₂O (20mL). The reaction was allowed to stir at room
42 temperature for 2 days and was then diluted with 1M HCl. The precipitate was filtered, washed
43 with H₂O, collected, and dried to afford **40** as an off-white solid (5.20 g, 96% yield). ¹H-NMR
44 (300 MHz, *d*₆-DMSO) δ 12.85 (br s, 1H), 11.09 (br s, 1H), 7.83-7.90 (m, 2H), 7.54 (d, *J* = 4.1
45 Hz, 1H), 7.19-7.28 (m, 3H); HPLC-1 = >99% (RT = 6.7 min).
46
47
48
49
50
51
52
53
54
55
56
57
58
59
60

41: 5-Chloro-*N*-(4-(5-nitrobenzo[d]oxazol-2-yl)phenyl)thiophene-2-sulfonamide.

Compound **40** (2.96 g, 9.31 mmol) was stirred in SOCl₂ (10 mL) for 6 h at 60°C, then was concentrated to a solid. This was refluxed with 2-amino-4-nitrophenol (2.96 g, 19.2 mmol) and pyridine (1.50 mL, 18.4 mmol) in anhydrous CH₂Cl₂ (50 mL) for 6 h, then stirred at R.T. for 3 days. The reaction was then extracted into EtOAc and rinsed with 1 M HCl and brine, dried over Na₂SO₄, filtered, and concentrated. This amide intermediate was then refluxed with TsOH•H₂O (3.61 g, 19.0 mmol) in xylenes (50 mL) using a Dean-Stark apparatus to remove the residual H₂O. After 18 h, the reaction was cooled, the xylenes decanted off, the sludge extracted with EtOAc, and the combined organics dried over Na₂SO₄, filtered, and concentrated. Flash chromatographic purification over silica (hexanes:EtOAc gradient) afforded **41** as a peach solid (1.81 g, 45% yield). ¹H-NMR (300 MHz, *d*₆-DMSO) δ 11.25 (br s, 1H), 8.64 (br s, 1H), 8.32 (d, *J* = 8.8 Hz, 1H), 8.18 (d, *J* = 8.1 Hz, 2H), 8.01 (d, *J* = 8.7 Hz, 1H), 7.60 (br s, 1H), 7.41 (d, *J* = 8.2 Hz, 2H), 7.24 (br s, 1H); MS (ESI) C₁₇H₁₁ClN₃O₅S₂ [M+H]⁺ *m/z* expected = 436.0, observed = 436.1; HPLC-1 = 88% (RT = 5.5 min).

42: *N*-(4-(5-Aminobenzo[d]oxazol-2-yl)phenyl)-5-chlorothiophene-2-sulfonamide.

Tin powder (1.53 g, 12.9 mmol) was added slowly to a stirring mixture of **41** (1.78 g, 4.08 mmol) in a 1:7 mixture of HCl:AcOH (8 mL). The reaction was stirred and heated at 60°C for 3 h, then cooled to R.T., diluted with EtOAc and H₂O, neutralized with NaHCO₃, and filtered. The filtrate was extracted with EtOAc and the organics dried over Na₂SO₄, filtered, and concentrated. The residue was diluted in a 10% mixture of DCM in hexanes and the precipitate was filtered, rinsed with hexanes, collected, and dried to afford **42** as a pale-yellow powder (1.59 g, 96% yield). ¹H-NMR (300 MHz, *d*₆-DMSO) δ 8.01-8.09 (m, 2H), 7.55 (d, *J* = 4.1 Hz, 1H),

1
2
3 7.30-7.41 (m, 3H), 7.22 (d, $J = 4.1$ Hz, 1H), 6.83 (d, $J = 2.0$ Hz, 1H), 6.64 (dd, $J = 8.7, 2.2$ Hz,
4 1H); MS (ESI) $C_{17}H_{13}ClN_3O_3S_2$ $[M+H]^+$ m/z expected = 406.0, observed = 406.1; HPLC-1 =
5
6 86% (RT = 6.8 min).
7
8
9
10
11

12 **General sulfonamidation procedure for the synthesis of 16L-34L.**

13
14 To a stirring mixture of compound **42** (1 eq.) in anhydrous CH_2Cl_2 (5 mL) was added the
15 respective R^2 sulfonyl chloride (1.2 eq.) followed by anhydrous pyridine (1.2 eq.). The reaction
16 was allowed to stir at room temperature for 18 h and was then chromatographed over silica
17 (hexanes:EtOAc gradient) and concentrated. If necessary, the product was further purified by
18 preparatory RP-HPLC ($H_2O:CH_3CN$ gradient), concentrated, and lyophilized. Refer to the
19 Supporting Information for individual compound synthesis and characterization data.
20
21
22
23
24
25
26
27
28
29
30

31 **Cell information for compound evaluation.**

32
33 The *ESKAPE* bacteria were purchased from the American Type Culture Collection
34 (ATCC): *E. faecium* (Orla-Jensen) Schleifer and Kilpper-Balz strain NCTC 7171 (ATCC
35 19434); *S. aureus* subsp. *aureus* Rosenbach strain Seattle 1945 (ATCC 25923); Multi-drug
36 resistant *S. aureus* (MRSA) subsp. *aureus* Rosenbach strain HPV107 (ATCC BAA-44); *K.*
37 *pneumonia*, subsp. *pneumoniae* (Schroeter) Trevisan strain NCTC 9633 (ATCC 13883); *A.*
38 *baumannii* Bouvet and Grimont strain 2208 (ATCC 19606); *P. aeruginosa* (Schroeter) Migula
39 strain NCTC 10332 (ATCC 10145); *E. cloacae*, subsp. *cloacae* (Jordan) Hormaeche and
40 Edwards strain CDC 442-68 (ATCC 13047). HEK 293 kidney cells (ATCC CRL-1573) and
41 THLE-3 liver cells (ATCC CRL-11233) were used for compound toxicity assays.
42
43
44
45
46
47
48
49
50
51
52
53
54
55
56
57
58
59
60

Evaluation of compounds for inhibition of bacterial cell proliferation.

All compounds were evaluated for inhibiting the proliferation of each of the *ESKAPE* bacteria as per previously reported procedures with one minor modification: Liquid growth media was cation-adjusted by addition of 25 mg/L Ca^{2+} and 12.5 mg/L Mg^{2+} to reflect the free concentrations of these divalent cations *in vivo*.²⁷ Detailed protocols for bacterial growth assays are presented in the Supporting Information.

Protein Expression and purification.

E. coli GroEL and GroES, and human HSP60 and HSP10, were expressed and purified as previously reported.²⁵ Detailed protocols for these protein purifications are presented in the Supporting Information.

Evaluation of compounds in GroEL/ES and HSP60/10-mediated dMDH and dRho refolding assays.

All compounds were evaluated for inhibiting *E. coli* GroEL/ES and human HSP60/10-mediated refolding of the denatured MDH and denatured Rho reporter enzymes as per previously reported procedures.²⁶ Detailed protocols for these assays are presented in the Supporting Information.

Counter-screening compounds for inhibition of native MDH and Rho enzymatic activity.

All compounds were counter-screened for inhibiting the enzymatic activity of the native MDH and native Rho reporter enzymes as per previously reported procedures.^{25, 26} Detailed protocols for the assays are presented in the Supporting Information.

1
2
3
4
5 **Evaluation of inhibitors 20R and 20L binding to GroEL using Isothermal Titration**
6 **Calorimetry (ITC).**
7

8
9
10 All ITC experiments were performed on a MicroCal VP-ITC system. To minimize
11 background heats of dilution, matched solutions of GroEL and compounds **20R** or **20L** were
12 prepared in buffer containing 20 mM HEPES, pH 7.4, 50 mM KCl, 10 mM MgCl₂, and 1%
13 DMSO. All buffers were freshly prepared from stock solutions on the day of use and degassed
14 under vacuum. For each analytical run, a solution of 400 μM GroEL (monomer concentration)
15 in the syringe was titrated into 50 μM solutions of either compound **20R** or **20L** in the sample
16 cell (equilibrated at 20°C for 300 seconds): the first injection was 0.4 μL (discarded during
17 analysis) and subsequent injections (2-20) were each 2.0 μL. Each injection was made over 4 s
18 durations with 3-min intervals between subsequent injections. The reference power of the
19 experiment was set to 6 μcal/s and a 5 s filter period. Sample stirring was set at 600 rpm for all
20 measurements. Six independent replicates were conducted to analyze compound **20R** binding,
21 and five replicates for **20L**. Raw thermograms from each replicate were analyzed independently
22 using the ORIGIN instrument software (MicroCal Inc., version 7.0). In each experiment, the
23 upper baseline was collected after the binding reaction was saturated, and the terminal 7-8 points
24 in the linear region were fit to a straight line and subtracted from the entire data set to remove
25 contributions from background heats of mixing and dilution. The ΔH was obtained by non-linear
26 least-squares fitting of the plot of ΔH (mol of injectant)⁻¹ versus molar ratio using a single site
27 binding model.³⁴ The ΔH, ΔS, K_d ($K_A = 1/K_d$), and binding stoichiometries (n) in each titration
28 were obtained, and ΔG was calculated using the Gibbs equation at a temperature of 20°C (293.15
29 K). Standard deviations were determined based on results from each of the replicate analyses.
30
31
32
33
34
35
36
37
38
39
40
41
42
43
44
45
46
47
48
49
50
51
52
53
54
55
56
57
58
59
60

Evaluation of compound effects on HEK 293 and THLE-3 cell viability.

Evaluation of compound cytotoxicities to HEK 293 kidney and THLE-3 liver cells were performed using Alamar Blue-based viability assays. HEK 293 cells were maintained in MEM medium (Corning Cellgro, 10-009 CV) supplemented with 10% FBS (Sigma, F2242). THLE-3 cells were maintained in Clonetics BEBM medium (Lonza, CC-3171) supplemented with the BEGM bullet kit (Lonza, CC-3170) and 10% FBS. All assays were carried out in 384-well plates (BRAND cell culture grade plates, 781980). Cells at 80% confluence were harvested and diluted in growth medium, then 45 μ L of the HEK 293 cells (1,500 cells/well) or THLE-3 cells (1,500 cells/well) were dispensed per well, and plates were sealed with "Breathe Easy" oxygen permeable membranes (Diversified Biotech) and incubated at 37°C, 5% CO₂, for 24 h. The following day, 1 μ L of the compound stocks (10 mM to 4.6 μ M, 3-fold dilutions in DMSO) were pre-diluted by pin-transfer into 25 μ L of the relevant growth mediums. Then, 15 μ L aliquots of the diluted compounds were added to the cell assay plates to give inhibitor concentration ranges of 100 μ M to 46 nM during the assay (final DMSO concentration of 0.1% was maintained during the assay). Plates were sealed with "Breathe Easy" oxygen permeable membranes and incubated for an additional 48 h at 37°C and 5% CO₂. The Alamar Blue reporter reagents were then added to a final concentration of 10%, the plates incubated at 37°C and 5% CO₂, and sample fluorescence (535 nm excitation, 590 nm emission) was read using a Molecular Devices FlexStation II 384-well plate reader (readings taken between 4-24 h of incubation so as to achieve signals in the 30-60% range for conversion of resazurin to resorufin). Cell viability was calculated as per vendor instructions (Thermo Fisher - Alamar Blue cell viability assay manual). Cytotoxicity CC₅₀ values for the test compounds were obtained by plotting the % resazurin

1
2
3 reduction results in GraphPad Prism 6 and analyzing by non-linear regression using the
4
5 log(inhibitor) vs. response (variable slope) equation. Results presented represent the averages of
6
7 CC_{50} values obtained from at least triplicate experiments.
8
9

13 **Evaluation of MRSA resistance generation against lead inhibitors.**

15 To identify potential resistance toward inhibitors, a liquid culture, 12-day serial passage
16 assay was employed as per procedures reported by Kim. S *et al.*, using the MRSA strain (ATCC
17 BAA-44).^{35,36} Briefly, MRSA bacteria were streaked onto a Tryptic Soy agar plate and grown
18 overnight at 37°C. A fresh aliquot of Tryptic Soy Broth (TSB) was inoculated with a single
19 bacterial colony and the cultures were grown overnight at 37°C with shaking (250 rpm). The
20 overnight culture was then sub-cultured (1:5 dilution) into a fresh aliquot of media and grown at
21 37°C for 1 h with shaking, then diluted into fresh media to achieve a final OD_{600} reading of 0.01.
22 Aliquots of the diluted culture (200 μ L) were dispensed to 96 well plates along with addition of 2
23 μ L of test compounds in DMSO (**20R**, **28R**, and vancomycin as a control). The inhibitor
24 concentration range during the resistance assay was 100 μ M to 48.8 nM (2-fold dilution series).
25 Plates were sealed with "Breathe Easy" oxygen permeable membranes (Diversified Biotech) and
26 left to incubate at 37°C without shaking (stagnant assay). OD_{600} readings were taken at the 24 h
27 time point to monitor for bacterial growth. A second set of baseline control plates were prepared
28 analogously, without any bacteria added, to correct for possible compound absorbance and/or
29 precipitation, as well as plate and media baseline effects. For inoculations on subsequent days,
30 bacteria from the wells with the highest drug concentration where the OD_{600} was >0.2 were
31 diluted with fresh media to OD_{600} of 0.01 and dispensed into a new 96-well plate. Test
32 compounds were added, and the bacteria propagated again as described above. This procedure
33
34
35
36
37
38
39
40
41
42
43
44
45
46
47
48
49
50
51
52
53
54
55
56
57
58
59
60

1
2
3 was repeated each day for a total of 12 days to observe changes in EC₅₀ values over each
4
5 passage. EC₅₀ values for the test compounds were obtained by plotting the OD₆₀₀ results from
6
7 each passage in GraphPad Prism 6 and analyzing by non-linear regression using the
8
9 log(inhibitor) vs. response (variable slope) equation. Results presented represent the averages of
10
11 EC₅₀ values obtained from at triplicate experiments.
12
13
14
15
16

17 **Calculation of IC₅₀ / EC₅₀ / CC₅₀ values and statistical considerations.**

18
19 All IC₅₀ / EC₅₀ / CC₅₀ results reported are averages of values determined from individual
20
21 dose-response curves in replicate assays as follows: 1) Individual I/E/CC₅₀ values from replicate
22
23 assays were first log-transformed and the average log(I/E/CC₅₀) values and standard deviations
24
25 (SD) calculated; 2) Replicate log(I/E/CC₅₀) values were evaluated for outliers using the ROUT
26
27 method in GraphPad Prism 6 (Q of 10%); and 3) Average I/E/CC₅₀ values were then back-
28
29 calculated from the average log(IC₅₀) values. To compare statistical differences between
30
31 log(I/E/CC₅₀) values between the matched **R**- and **L**-series of analogs, two-tailed, paired t-tests
32
33 were performed using GraphPad Prism 6 (95% confidence level) and looking at differences
34
35 between paired values (results are plotted in **Figures S1-S5** in the Supporting Information). For
36
37 compounds where log(I/E/CC₅₀) values were greater than the maximum compound
38
39 concentrations tested (i.e. >1.8 and >2.0, or >63 and >100 μM, respectively), results were
40
41 represented as 0.1 log units higher than the maximum concentrations tested (i.e. 1.9 and 2.1, or
42
43 79 and 126 μM, respectively), so as not to overly bias comparisons because of the unavailability
44
45 of definitive values for these inactive compounds.
46
47
48
49
50
51
52
53

54 **Corresponding Author**

* E-mail: johnstm@iu.edu, Phone: 317-274-2458, Fax: 317-274-4686.

ACKNOWLEDGMENTS.

Research reported in this publication was supported by the National Institute of General Medical Sciences (NIGMS) of the National Institutes of Health (NIH) under Award Number R01GM120350. QQH and YP additionally acknowledge support by NIH grants 5R01GM111639 and 5R01GM115844. The content is solely the responsibility of the authors and does not necessarily represent the official views of the NIH. This work was also supported, in part, by the Howard Hughes Medical Institute (AH), an IU Biomedical Research Grant (SMJ), and startup funds from the IU School of Medicine (SMJ) and the University of Arizona (EC). The human HSP60 expression plasmid (lacking the 26 amino acid *N*-terminal mitochondrial signal peptide) was generously donated by Dr. Abdussalam Azem from Tel Aviv University, Faculty of Life Sciences, Department of Biochemistry, Israel.

ABBREVIATIONS.

MDH, malate dehydrogenase; Rho, rhodanese; HPLC, high-performance liquid chromatography; ¹H-NMR, Proton nuclear magnetic resonance; MS, Mass spectrometry; EtOH, ethanol; AcOH, acetic acid; EtOAc, ethyl acetate; MeOH, methanol; DMSO, dimethyl sulfoxide; IC₅₀ - Inhibitory concentration for half-maximal signal in biochemical assay; EC₅₀, effective concentration for half-maximal signal in bacterial proliferation assays; CC₅₀, cytotoxicity concentration for half-maximal signal in human cell viability assays; ITC, isothermal titration calorimetry.

Supporting Information.

Supporting information associated with this article can be found in the online version, which includes tabulation of all biochemical IC_{50} , bacterial proliferation EC_{50} , and human cell viability CC_{50} results; $\log(IC_{50})$, $\log(EC_{50})$, and $\log(CC_{50})$ results with standard deviations; plots of statistical differences between the **R**- and **L**-series analogs in the various assays; synthetic protocols and characterization data for test compounds (HPLC purity, MS, and 1H -NMR); experimental protocols for protein synthesis and purification, and biochemical, bacterial proliferation, and human cell viability assays; and SMILES strings of compound structures.

REFERENCES

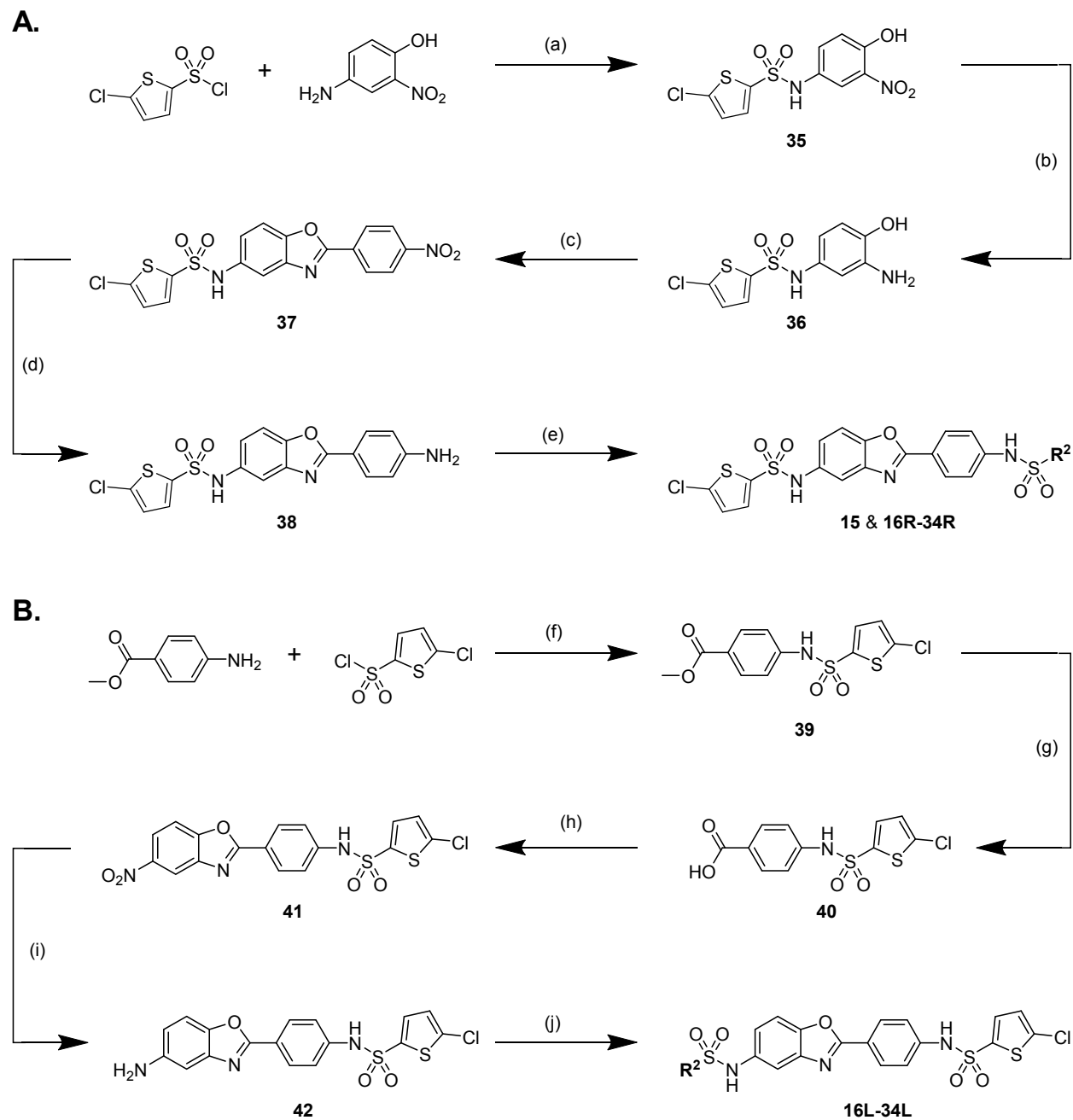
1. Tacconelli, E.; Magrini, N. *Global priority list of antibiotic-resistant bacteria to guide research, discovery, and development of new antibiotics*. World Health Organization: Geneva, Switzerland, 2017; p 7.
2. Centers for Disease Control and Prevention. *Antibiotic Resistance Threats in the United States, 2013*. Centers for Disease Control and Prevention: Atlanta, Georgia, USA, 2013; p 114.
3. Karlowsky, J. A.; Hoban, D. J.; Hackel, M. A.; Lob, S. H.; Sahm, D. F. Antimicrobial susceptibility of Gram-negative ESKAPE pathogens isolated from hospitalized patients with intra-abdominal and urinary tract infections in Asia-Pacific countries: SMART 2013-2015. *J. Med. Microbiol.* **2017**, 66, 61-69.
4. Santajit, S.; Indrawattana, N. Mechanisms of antimicrobial resistance in ESKAPE pathogens. *Biomed. Res. Int.* **2016**, 2016, 2475067.
5. Rice, L. B. Federal funding for the study of antimicrobial resistance in nosocomial pathogens: No ESKAPE. *J. Infect. Dis.* **2008**, 197, 1079-1081.
6. Choo, E. J.; Chambers, H. F. Treatment of methicillin-resistant *Staphylococcus aureus* bacteremia. *Infect. Chemother.* **2016**, 48, 267-273.
7. Hassoun, A.; Linden, P. K.; Friedman, B. Incidence, prevalence, and management of MRSA bacteremia across patient populations-a review of recent developments in MRSA management and treatment. *Crit. Care* **2017**, 21, 211.
8. Boucher, H.; Miller, L. G.; Razonable, R. R. Serious infections caused by methicillin-resistant *Staphylococcus aureus*. *Clin. Infect. Dis.* **2010**, 51 Suppl 2, S183-197.

- 1
2
3 9. Wong, P.; Houry, W. A. Chaperone networks in bacteria: analysis of protein homeostasis in
4 minimal cells. *J. Struct. Biol.* **2004**, 146, 79-89.
5
6
- 7
8 10. Mogk, A.; Huber, D.; Bukau, B. Integrating protein homeostasis strategies in prokaryotes.
9
10 *Cold Spring Harb. Perspect. Biol.* **2011**, 3.
11
- 12 11. Chiappori, F.; Fumian, M.; Milanesi, L.; Merelli, I. DnaK as antibiotic target: Hot spot
13 residues analysis for differential inhibition of the bacterial protein in comparison with the
14 human HSP70. *PLoS One* **2015**, 10, e0124563.
15
16
- 17 12. Arita-Morioka, K.; Yamanaka, K.; Mizunoe, Y.; Ogura, T.; Sugimoto, S. Novel strategy for
18 biofilm inhibition by using small molecules targeting molecular chaperone DnaK.
19
20 *Antimicrob. Agents Chemother.* **2015**, 59, 633-641.
21
22
- 23 13. Sass, P.; Josten, M.; Famulla, K.; Schiffer, G.; Sahl, H. G.; Hamoen, L.; Brotz-Oesterhelt, H.
24 Antibiotic acyldepsipeptides activate ClpP peptidase to degrade the cell division protein
25
26 FtsZ. *Proc. Natl. Acad. Sci. U.S.A.* **2011**, 108, 17474-17479.
27
28
- 29 14. Evans, C. G.; Chang, L.; Gestwicki, J. E. Heat shock protein 70 (hsp70) as an emerging drug
30 target. *J. Med. Chem.* **2010**, 53, 4585-4602.
31
32
- 33 15. Braig, K.; Otwinowski, Z.; Hegde, R.; Boisvert, D. C.; Joachimiak, A.; Horwich, A. L.;
34
35 Sigler, P. B. The crystal structure of the bacterial chaperonin GroEL at 2.8 Å. *Nature* **1994**,
36
37 371, 578-586.
38
39
- 40 16. Sigler, P. B.; Xu, Z.; Rye, H. S.; Burston, S. G.; Fenton, W. A.; Horwich, A. L. Structure and
41
42 function in GroEL-mediated protein folding. *Annu. Rev. Biochem.* **1998**, 67, 581-608.
43
44
- 45 17. Horwich, A. L.; Farr, G. W.; Fenton, W. A. GroEL-GroES-mediated protein folding. *Chem.*
46
47 *Rev.* **2006**, 106, 1917-1930.
48
49
50
51
52
53
54
55
56
57
58
59
60

- 1
2
3 18. Fenton, W. A.; Kashi, Y.; Furtak, K.; Horwich, A. L. Residues in chaperonin GroEL required
4
5 for polypeptide binding and release. *Nature* **1994**, 371, 614-619.
6
7
8 19. Fenton, W. A.; Horwich, A. L. GroEL-mediated protein folding. *Protein Sci.* **1997**, 6, 743-
9
10 760.
11
12 20. Horwich, A. L.; Fenton, W. A.; Chapman, E.; Farr, G. W. Two families of chaperonin:
13
14 physiology and mechanism. *Annu. Rev. Cell. Dev. Biol.* **2007**, 23, 115-145.
15
16
17 21. Saibil, H. R.; Fenton, W. A.; Clare, D. K.; Horwich, A. L. Structure and allostery of the
18
19 chaperonin GroEL. *J. Mol. Biol.* **2013**, 425, 1476-1487.
20
21
22 22. Chapman, E.; Farr, G. W.; Usaite, R.; Furtak, K.; Fenton, W. A.; Chaudhuri, T. K.; Hondorp,
23
24 E. R.; Matthews, R. G.; Wolf, S. G.; Yates, J. R.; Pypaert, M.; Horwich, A. L. Global
25
26 aggregation of newly translated proteins in an Escherichia coli strain deficient of the
27
28 chaperonin GroEL. *Proc. Natl. Acad. Sci. U.S.A.* **2006**, 103, 15800-15805.
29
30
31 23. Fayet, O.; Ziegelhoffer, T.; Georgopoulos, C. The groES and groEL heat shock gene
32
33 products of Escherichia coli are essential for bacterial growth at all temperatures. *J.*
34
35 *Bacteriol.* **1989**, 171, 1379-1385.
36
37
38 24. Johnson, S. M.; Sharif, O.; Mak, P. A.; Wang, H. T.; Engels, I. H.; Brinker, A.; Schultz, P.
39
40 G.; Horwich, A. L.; Chapman, E. A biochemical screen for GroEL/GroES inhibitors. *Bioorg.*
41
42 *Med. Chem. Lett.* **2014**, 24, 786-789.
43
44
45 25. Abdeen, S.; Salim, N.; Mammadova, N.; Summers, C. M.; Frankson, R.; Ambrose, A. J.;
46
47 Anderson, G. G.; Schultz, P. G.; Horwich, A. L.; Chapman, E.; Johnson, S. M. GroEL/ES
48
49 inhibitors as potential antibiotics. *Bioorg. Med. Chem. Lett.* **2016**, 26, 3127-3134.
50
51
52 26. Abdeen, S.; Salim, N.; Mammadova, N.; Summers, C. M.; Goldsmith-Pestana, K.;
53
54 McMahan-Pratt, D.; Schultz, P. G.; Horwich, A. L.; Chapman, E.; Johnson, S. M. Targeting
55
56
57
58
59
60

- 1
2
3 the HSP60/10 chaperonin systems of *Trypanosoma brucei* as a strategy for treating African
4 sleeping sickness. *Bioorg. Med. Chem. Lett.* **2016**, 26, 5247-5253.
5
6
7
8 27. Wiegand, I.; Hilpert, K.; Hancock, R. E. Agar and broth dilution methods to determine the
9 minimal inhibitory concentration (MIC) of antimicrobial substances. *Nat. Protoc.* **2008**, 3,
10 163-175.
11
12
13
14 28. Johnson, S. M.; Connelly, S.; Wilson, I. A.; Kelly, J. W. Toward optimization of the linker
15 substructure common to transthyretin amyloidogenesis inhibitors using biochemical and
16 structural studies. *J. Med. Chem.* **2008**, 51, 6348-6358.
17
18
19
20 29. Connelly, S.; Mortenson, D. E.; Choi, S.; Wilson, I. A.; Powers, E. T.; Kelly, J. W.; Johnson,
21 S. M. Semi-quantitative models for identifying potent and selective transthyretin
22 amyloidogenesis inhibitors. *Bioorg. Med. Chem. Lett.* **2017**, 27, 3441-3449.
23
24
25
26 30. Johnson, S. M.; Connelly, S.; Wilson, I. A.; Kelly, J. W. Toward optimization of the second
27 aryl substructure common to transthyretin amyloidogenesis inhibitors using biochemical and
28 structural studies. *J. Med. Chem.* **2009**, 52, 1115-1125.
29
30
31
32
33 31. Tipparaju, S. K.; Joyasawal, S.; Pieroni, M.; Kaiser, M.; Brun, R.; Kozikowski, A. P. In
34 pursuit of natural product leads: Synthesis and biological evaluation of 2-[3-hydroxy-2-[(3-
35 hydroxypyridine-2-carbonyl)amino]phenyl]benzoxazole-4-carboxylic acid (A-33853) and its
36 analogues: Discovery of N-(2-benzoxazol-2-ylphenyl)benzamides as novel antileishmanial
37 chemotypes. *J. Med. Chem.* **2008**, 51, 7344-7347.
38
39
40
41
42 32. Wiseman, R. L.; Johnson, S. M.; Kelker, M. S.; Foss, T.; Wilson, I. A.; Kelly, J. W. Kinetic
43 stabilization of an oligomeric protein by a single ligand binding event. *J. Am. Chem. Soc.*
44 **2005**, 127, 5540-5551.
45
46
47
48
49
50
51
52
53
54
55
56
57
58
59
60

- 1
2
3 33. Johnson, S. M.; Connelly, S.; Wilson, I. A.; Kelly, J. W. Biochemical and structural
4 evaluation of highly selective 2-arylbenzoxazole-based transthyretin amyloidogenesis
5 inhibitors. *J. Med. Chem.* **2008**, 51, 260-270.
6
7
8
9
10 34. Wiseman, T.; Williston, S.; Brandts, J. F.; Lin, L. N. Rapid measurement of binding
11 constants and heats of binding using a new titration calorimeter. *Anal. Biochem.* **1989**, 179,
12 131-137.
13
14
15
16
17 35. Kim, S.; Lieberman, T. D.; Kishony, R. Alternating antibiotic treatments constrain
18 evolutionary paths to multidrug resistance. *Proc. Natl. Acad. Sci. U.S.A.* **2014**, 111, 14494-
19 14499.
20
21
22
23
24 36. Fleeman, R.; LaVoi, T. M.; Santos, R. G.; Morales, A.; Nefzi, A.; Welmaker, G. S.; Medina-
25 Franco, J. L.; Giulianotti, M. A.; Houghten, R. A.; Shaw, L. N. Combinatorial libraries as a
26 tool for the discovery of novel, broad-spectrum antibacterial agents targeting the ESKAPE
27 pathogens. *J. Med. Chem.* **2015**, 58, 3340-3355.
28
29
30
31
32
33
34
35
36
37
38
39
40
41
42
43
44
45
46
47
48
49
50
51
52
53
54
55
56
57
58
59
60

Schemes, Figures, and Tables.**Scheme 1^a**

1
2
3 ^a Reagents and conditions: **A.** (a) CH₂Cl₂, rt (94%); (b) tin powder, 10% HCl in AcOH, rt (82%);
4
5 (c) 4-nitrobenzaldehyde, NaHCO₃, Na₂SO₄, THF, reflux to rt, then DDQ added (95%); (d) tin
6
7 powder, 10% HCl in AcOH, rt (41%); (e) **R**²-SO₂Cl, pyridine, CH₂Cl₂, rt. **B.** (f) CH₂Cl₂, rt
8
9 (98%); (g) LiOH•H₂O, 1:1:1 THF:MeOH:H₂O, rt (96%); (h) SOCl₂, 60°C for 1 h, concentrated,
10
11 then 2-amino-4-nitrophenol and pyridine in CH₂Cl₂, reflux to rt, then TsOH•H₂O, xylenes, reflux
12
13 (45%); (i) tin powder, 10% HCl in AcOH, rt (96%); (j) **R**²-SO₂Cl, pyridine, CH₂Cl₂, rt.
14
15
16
17
18
19
20
21
22
23
24
25
26
27
28
29
30
31
32
33
34
35
36
37
38
39
40
41
42
43
44
45
46
47
48
49
50
51
52
53
54
55
56
57
58
59
60

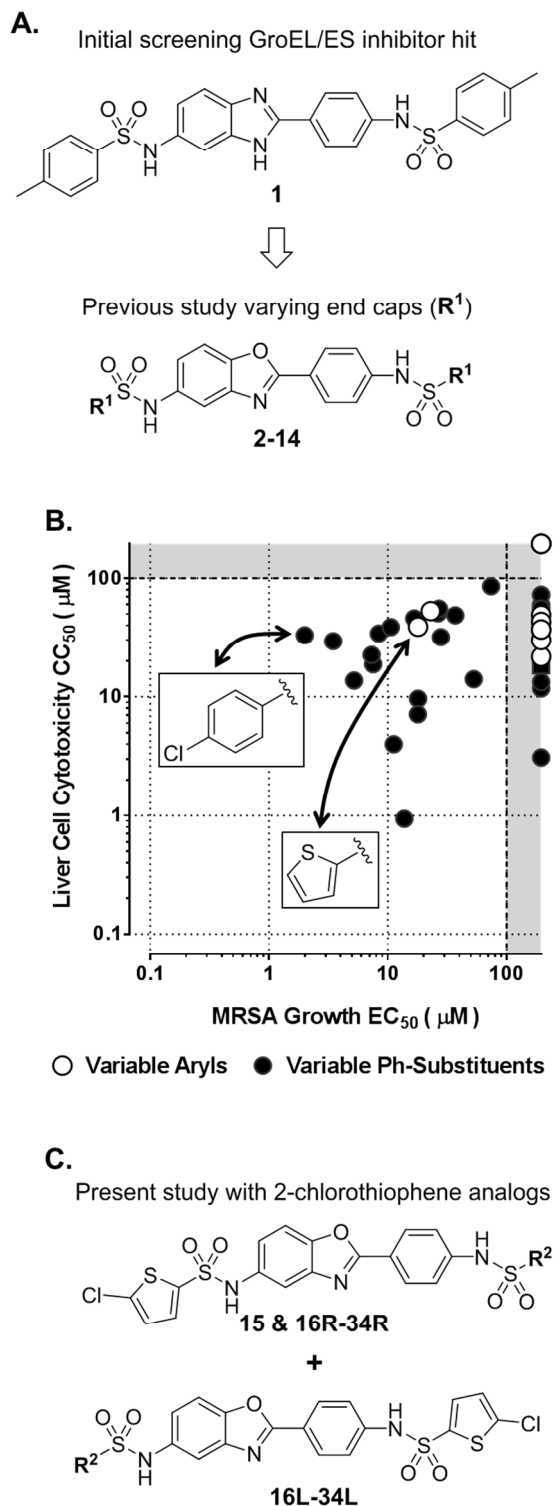


Figure 1. Progression of hit-to-lead compound **1** analogs. **A.** Compound **1** was an initial hit that emerged from our high-throughput screening for GroEL/ES inhibitors.²⁴ We recently reported

1
2
3 on a series of pseudo-symmetrical compound **1** analogs (**2-14** – R^1 represents a variety of alkyl,
4 aryl, and substituted phenyl substructures) that have antibiotic properties against *Trypanosoma*
5 *brucei* parasites.²⁶ **B.** In the present study, we initially screened the **1-14** analogs for their ability
6 to inhibit a panel of Gram-positive and Gram-negative bacteria, and found that the thiophene (**6**)
7 and *para*-chloro-substituted (**2c-p**) analogs generated the most potent and selective inhibitors of
8 MRSA proliferation. Data plotted in the gray zones represent EC₅₀ and CC₅₀ results beyond the
9 assay detection limits (i.e., >100 μM). **C.** Based on initial SAR, compound **15** was developed
10 (bearing the 2-chlorothiophene group on both sides) along with two parallel series of
11 asymmetrical 2-chlorothiophene-based analogs (**16-34**, **Right** and **Left**) containing variable alkyl
12 and aryl substructures at the R^2 positions were developed in an attempt to improve their
13 selectivity indices between efficacy against bacterial proliferation and cytotoxicity in human cell
14 viability assays (structures of the different R^2 groups are presented in **Tables S3A** and **S4A** in
15 the Supporting Information).
16
17
18
19
20
21
22
23
24
25
26
27
28
29
30
31
32
33
34
35
36
37
38
39
40
41
42
43
44
45
46
47
48
49
50
51
52
53
54
55
56
57
58
59
60

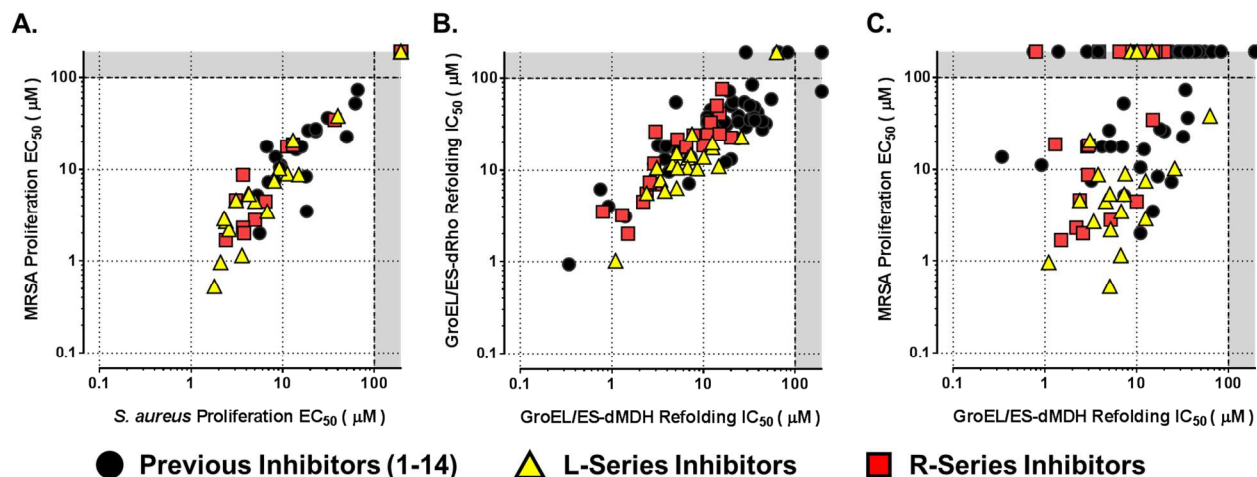


Figure 2. Correlation plots of IC₅₀ and EC₅₀ values for compounds tested in the respective GroEL/ES-dMDH or dRho refolding assays and bacterial proliferation assays. Each data point represents results for individual compounds tested in the respective assays (plotted from results presented in **Tables S1-S4** in the Supporting Information). Data plotted in the gray zones represent results beyond the assay detection limits (i.e., >100 µM). **A.** Compounds inhibit the proliferation of *S. aureus* (drug susceptible) and MRSA (drug resistant) bacteria nearly equipotently. The **L-** and **R-**series asymmetric inhibitors are generally more potent than the previously developed pseudo-symmetrical inhibitors (**1-14**). **B.** Compounds are on-target for inhibiting chaperonin-mediated substrate refolding as a correlation is evident between IC₅₀ values obtained from the GroEL/ES-dMDH and -dRho refolding assays, and compounds do not inhibit in both the native MDH and Rho enzymatic activity counter-screens. **C.** A general trend is observed between inhibiting the GroEL/ES chaperonin system and MRSA proliferation, supporting on-target effects in bacteria.

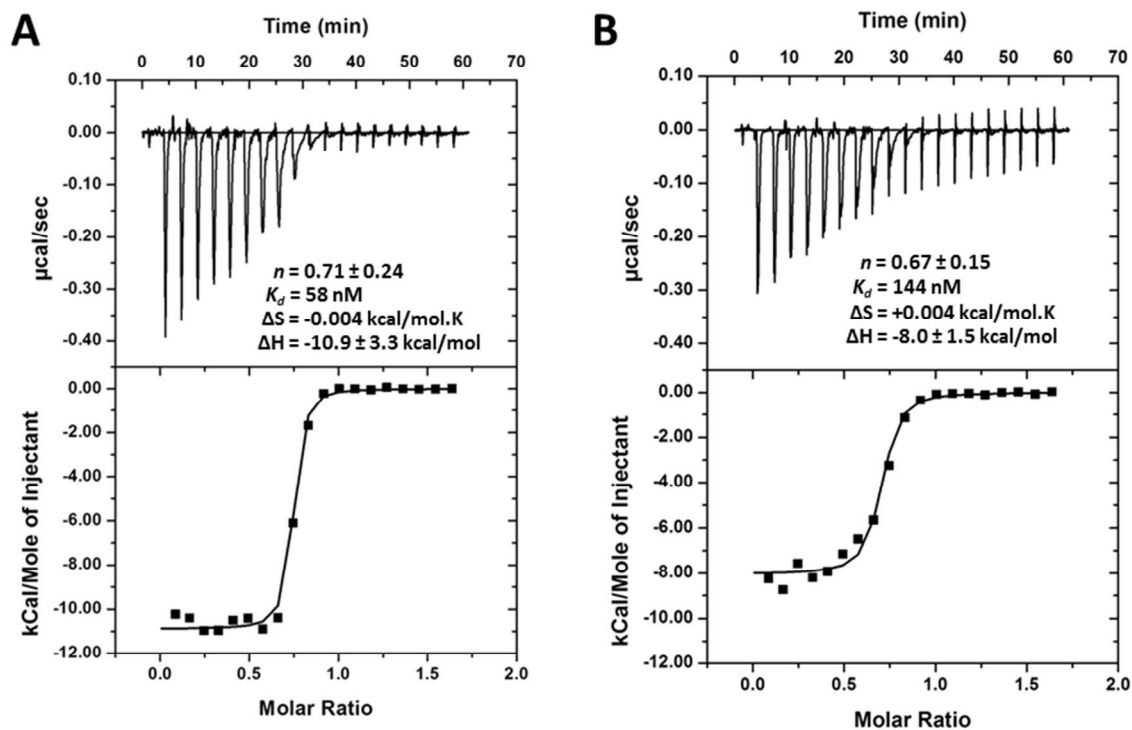


Figure 3. Representative analyses of the binding of **20R** (Panel **A**) and **20L** (Panel **B**) to GroEL measured by Isothermal Titration Calorimetry (ITC). Top panels show binding isotherms obtained by titrating GroEL (400 μM monomer concentration) into solutions of either **20R** or **20L** (50 μM) in the ITC cell. Lower panels show the integrated data (solid squares) fit to a single-site binding model (solid lines). The molar ratio refers to the binding stoichiometry of monomeric GroEL to molecules **20R** or **20L**. Average results for the various binding parameters (K_d , n , ΔH , ΔS , and ΔG) obtained from replicate analyses are presented in **Table 1**.

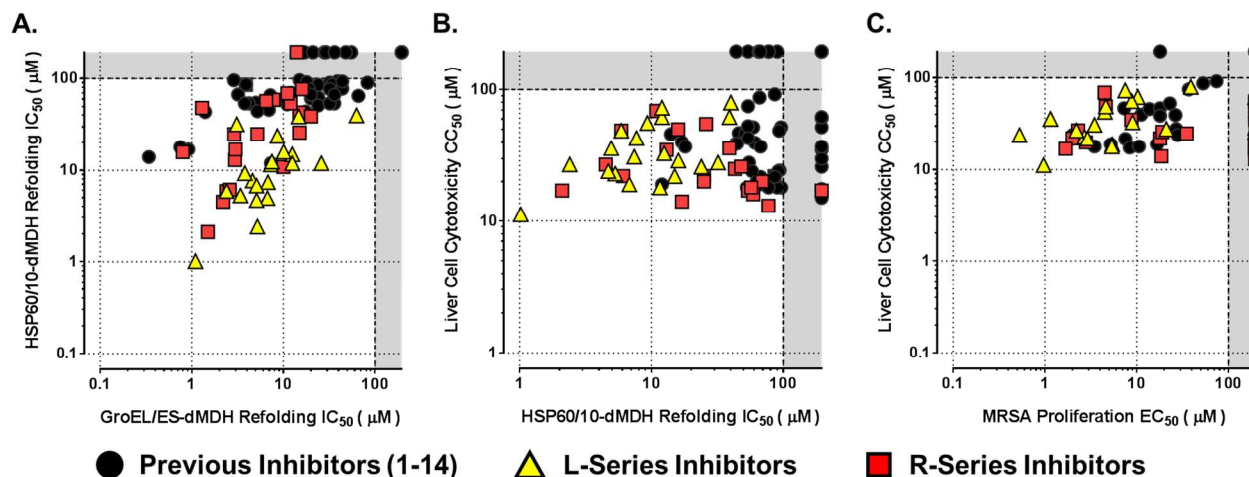


Figure 4. Correlation plots of IC_{50} , EC_{50} , and CC_{50} values for compounds tested in the respective GroEL/ES-dMDH and HSP60/10-dMDH refolding assays, liver cell cytotoxicity assay, and MRSA proliferation assay. Each data point represents results for individual compounds tested in the respective assays (plotted from results presented in **Tables S1-S4** in the Supporting Information). Data plotted in the gray zones represent results beyond the assay detection limits (i.e., >100 µM). **A.** The **R**-series and previously developed analogs selectively inhibit the *E. coli* GroEL/ES over the human HSP60/10 chaperonin system, but the **L**-series analogs are not selective. **B.** No correlation is evident between cytotoxicity of compounds in the liver cell viability assay and the HSP60/10-dMDH refolding assay, suggesting cytotoxicity may be from off-target effects in cells. **C.** Many compounds are able to selectively inhibit MRSA proliferation with moderate to low cytotoxicity to human liver cells. Results are similar for compounds tested in the kidney cell viability assay.

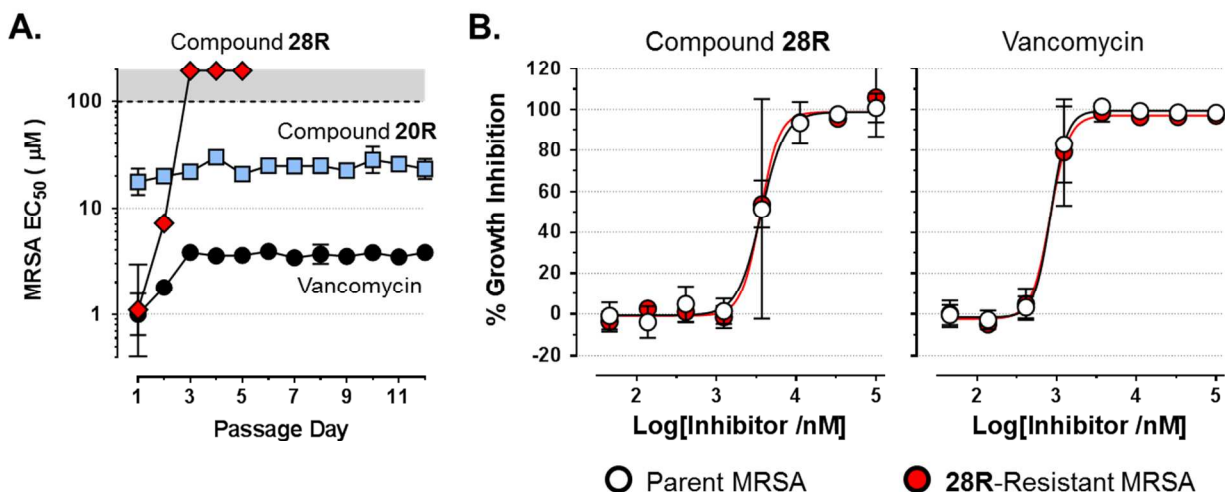


Figure 5. Exploring adaptive tolerance by MRSA bacteria to analogs **20R**, **28R**, and vancomycin. **A.** MRSA was serially passaged for 12 days in fresh liquid media supplemented with the selected compounds. Average EC₅₀ values of compounds tested after each 24 h passage are plotted from triplicate analyses. MRSA rapidly evolved resistance to **28R**, but retained sensitivity to **20R** and vancomycin throughout 12 day experiment. Data plotted in the gray zones represent EC₅₀ results beyond the assay detection limits (i.e., >100 µM). **B.** After re-culturing the **28R**-resistant MRSA strain for two days in the absence of inhibitors (24 h on agar, then another 24 h in liquid medium), the “resistant” MRSA strain regained sensitivity to **28R** (average % growth inhibition results (±SD) are plotted from 4 replicate analyses).

Table 1. Isothermal Titration Calorimetry (ITC) results for compounds **20R** and **20L**. Results are averaged from six replicate analyses for **20R**, and five replicate analyses for **20L**.

		20R	20L
Assay IC ₅₀ (μM)	GroEL/ES-dMDH Refolding	1.3	3.1
	GroEL/ES-dRho Refolding	3.2	11
Stoichiometry n	GroEL _{monomer} : Molecule	0.77 ± 0.16	0.6 ± 0.14
	Molecule : GroEL _{monomer}	1.30 ± 0.27	1.67 ± 0.39
	Molecule : GroEL _{oligomer}	18.2 ± 3.8	23.3 ± 5.4
Log(K _d /nM)		1.56 ± 0.20	2.18 ± 0.03
K _d (nM)		36	150
ΔH (kcal/mol)		-9.78 ± 0.80	-8.30 ± 0.52
ΔS (kcal/mol·K)		0.001 ± 0.003	0.003 ± 0.002
TΔS (kcal/mol)		0.20 ± 0.82	0.84 ± 0.55
ΔG (kcal/mol)		-9.98 ± 0.26	-9.14 ± 0.06

Table 2. Biochemical and cell-based IC₅₀, EC₅₀, and CC₅₀ results for the top four lead inhibitors based on Selectivity Index (SI) for inhibiting MRSA proliferation over cytotoxicity in the liver cell viability assay.

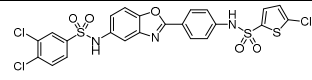
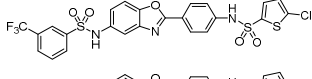
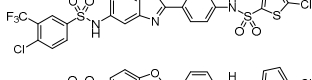
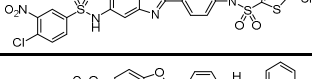
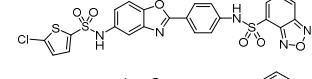
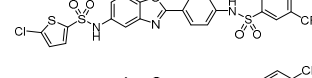
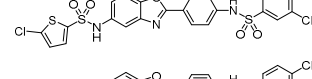
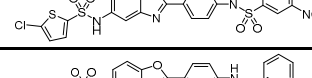
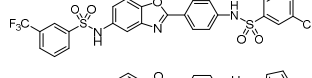
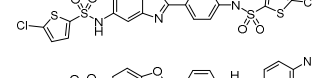
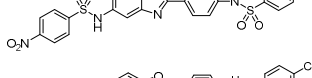
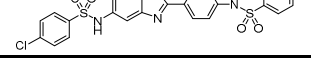
Compound Structure & Number	Cell-Based Assays			Biochemical Assay IC ₅₀ (μM)					
	MRSA Proliferation EC ₅₀ (μM)	Liver Cell Viability CC ₅₀ (μM)	Selectivity Index (SI) (CC ₅₀ / EC ₅₀)	Native Rho Reporter	Native MDH Reporter	GroEL/ES refolding of:		HSP60/10-dMDH Refolding	
						dRho	dMDH		
L-Series Analogs    	25L	0.53	24	46	>100	>63	6.4	5.1	4.7
	24L	1.1	36	31	>100	43	11	6.7	5.0
	27L	2.2	27	12	>100	40	11	5.2	2.4
	28L	0.97	11	12	>100	37	1.0	1.1	1.0
R-Series Analogs    	33R	4.5	69	15	72	>63	19	10.0	11
	24R	2.3	27	12	>100	>63	4.5	2.2	4.5
	27R	2.0	22	11	>100	>63	7.3	2.6	6.1
	28R	1.7	17	10	53	34	2.0	1.5	2.1
Pseudo-symmetrical Analogs    	2f-m	2.0	24	12	>100	>63	33	11	58
	15	4.6	49	11	>100	52	5.6	2.4	5.9
	2i-p	7.3	47	6.4	>100	>63	22	24	51
	2c-p	3.5	18	5.2	>100	>63	29	15	96

Table 3. Comparison of the **L-** and **R-**series analogs for which overall scaffolds exhibited preferred inhibition profiles in the various biochemical and cell-based assays. Lead antibacterial candidates are preferred to potently inhibit GroEL/ES and bacteria, and not inhibit human HSP60/10 and liver/kidney cell viability. The $\log(\text{IC}_{50})$, $\log(\text{EC}_{50})$, or $\log(\text{CC}_{50})$ values for the 20 matched **L-** and **R-**series analogs were analyzed by two-tailed, paired t-tests with 95% confidence intervals. Comparative plots are presented in **Figures S1-S5** in the Supporting Information.

Assay Inhibition	L-Series	R-Series
<i>S. aureus</i> growth	Preferred	
MRSA growth	Preferred	
GroEL/ES-dMDH refolding	No statistical difference	
GroEL/ES-dRho refolding	No statistical difference	
HSP60/10-dMDH refolding		Preferred
Liver cell viability	Preferred	
Kidney cell viability	No statistical difference	

Table of Contents Graphic.